ELSEVIER

Intermetallics 7 (1999) 543–551

Intermetallics

Influence of grain boundary composition on the moisture-induced embrittlement of $Ni_3(Si,Ti)$ alloys

T. Takasugi*, C.T. Liu, L. Heatherly, E.H. Lee, E.P. George

Metals and Ceramics Division, Oak Ridge National Laboratory, TN 37831-6093, USA

Received 15 June 1998; accepted 26 June 1998

Abstract

$Ni_3(Si,Ti)$ alloys containing different levels of boron were tensile tested in air at room temperature at two different strain rates. The grain boundary compositions and fracture modes of these alloys were determined by Auger spectroscopy and scanning electron microscopy, respectively. Tensile elongation and fracture mode depend upon the fabrication procedure, heat treatment, and strain rate. Widely different boron concentrations were observed at the grain boundaries, depending on the fabrication procedure and heat treatment. In addition, silicon and titanium were depleted while nickel was enriched at the grain boundaries in all specimens examined. Tensile elongations correlated well with the grain boundary concentration of boron and also with an embrittlement parameter defined as (Si + Ti − B)/Ti. A sharp brittle-ductile transition was found to occur with increasing grain boundary concentration of boron and with decreasing values of the embrittlement parameter (Si + Ti − B)/Ti. The critical grain boundary concentrations corresponding to this transition were found to be sensitive to the strain rate. All the results can be explained in terms of the effect of grain-boundary composition on moisture-induced environmental embrittlement. © 1999 Elsevier Science Ltd. All rights reserved.

Keywords: A. Silicides, various; B. Environmental embrittlement; C. Interstitial content; control; D. Grain boundaries; structure; F. Spectroscopic methods, various

1. Introduction

Titanium has the largest solubility limit (~11 at%) in the $L1_2$ Ni_3Si phase, except for Al, Ga and Ge, which substitute for Si and form continuous solid solutions up to their respective terminal $L1_2$ phases of Ni_3Al, Ni_3Ga and Ni_3Ge [1,2]. Titanium also substitutes for Si in Ni_3Si and stabilizes the $L1_2$ structure up to its melting point [1]. The effects of Ti on the mechanical properties of Ni_3Si have been well characterized using polycrystals and single-crystals [3–5]. Ti additions to Ni_3Si resulted in increased strength accompanied by high tensile ductility over a wide range of temperatures [3]. Also, Ti additions enhanced the peak temperature in the strength versus temperature curve [5]. Thus, the $Ni_3(Si,Ti)$ alloys have a number of useful mechanical properties. However, the $Ni_3(Si,Ti)$ alloys have been known to exhibit the so-called environmental embrittlement [3,4,6] like other intermetallic alloys with the $L1_2$-type structure (such as Ni_3Al and Co_3Ti) [7–9]. The $Ni_3(Si,Ti)$ alloys exhibited substantially reduced tensile ductility and intergranular fracture when tested in air or hydrogen-containing environments at ambient temperatures. The environmental embrittlement of the $Ni_3(Si,Ti)$ alloys is primarily due to atomic hydrogen produced by a reaction of Si and Ti with moisture in air and the subsequent hydrogen penetration near the crack tips. Also, it has been shown by Takasugi et al. that the environmental embrittlement of the $Ni_3(Si,Ti)$ alloys is significantly affected by the alloy composition as well as experimental conditions (i.e. atmosphere, temperature and deformation rate) [3,4,6,10]. For example, doping with a trace amount of boron almost completely suppresses the environmental embrittlement of the $Ni_3(Si,Ti)$ alloys [6,10,11]. It was suggested that boron segregating at the grain boundaries (as detected by field ion microscopic observations (FIM) [12]) probably prohibits the harmful action of the hydrogen atoms at the grain boundaries [3,4,6,10] Similarly, ternary elements such as Cr, Mn

* Corresponding author permanent address at: Institute for Materials Research, Tohoku University, Katahira 2-1-1, Aoba-ku, Sendai 980-8577, Japan. Tel.: +81-22-215-2117; fax: +81-22-215-2116

0966-9795/99/$—see front matter © 1999 Elsevier Science Ltd. All rights reserved
PII: S0966-9795(98)00072-7

and Fe at levels of a couple of atomic percent have the effect of substantially reducing the environmental embrittlement of the $Ni_3(Si,Ti)$ alloys [13,14]. Among those transition elements, chromium was shown to be the most effective in reducing the embrittlement of the $Ni_3(Si,Ti)$ alloys in air as well as in distilled water [14], although a recent study by Kumar et al. did not support this conclusion [15]. It was suggested that ternary alloying elements affect the decomposition process on the material surface or the subsequent kinetics, although no clear direct evidence or mechanism is yet available.

It is possible that ternary alloying elements may significantly influence grain boundary compositions, thereby affecting the atomic hydrogen production and penetration along the grain boundaries as well as intergranular cohesion. A first attempt to study grain boundary compositions using Auger instrument was done recently on $Ni_3(Si,Ti)$ alloys unintentionally doped with boron [16]. It was observed that the grain boundary compositions were different from that in the grain interiors, and the environmental embrittlement of $Ni_3(Si,Ti)$ alloys could be correlated with the embrittlement factor defined as $(Si+Ti)/Ti$ [16]. However, in the previous work, the boron doping levels were limited and not well controlled because it was unintentionally doped (i.e. contaminated) [16]. The boron contamination and its source have recently been characterized in detail, and the results will be published elsewhere [17].

In this study, we used $Ni_3(Si,Ti)$ alloys in which the boron concentration as well as the concentrations of the constituent elements were well controlled. Also, $Ni_3(Si,Ti)$ alloys containing a wide range of boron concentration were used in this study. Mechanical properties were characterized in air by tensile tests. To study the grain boundary compositions and fracture modes of the $Ni_3(Si,Ti)$ alloys, scanning Auger microscopy and scanning electron microscopy (SEM) were used, respectively. The tensile elongation in air is correlated with the measured grain boundary compositions, and discussed in terms of the environmental embrittlement.

2. Experimental procedure

Three alloys of $Ni_3(Si,Ti)$ with the same nominal composition of 79.5 at%Ni, 11.0 at%Si and 9.5 at%Ti were used in this work. One alloy was made at the Oak Ridge National Laboratory (ORNL) (referred to as alloy 200) and the other two alloys were made at the Institute for Materials Research at Tohoku University (referred to as alloys 712 and 713). Among these alloys, only alloy 713 was intentionally doped with 50 wt ppm boron, using a master alloy consisting of Ni–10 wt% boron. The alloy 200 was made by arc melting and drop casting, while the alloys 713 and 712 were simply arc melted and allowed to solidify into a button. The detailed procedures for fabricating the three alloys into tensile specimens have been described elsewhere [15,16]. Repeated cold rolling with intermediate annealing (at high temperature in vacuum) was used to produce sheet specimens, except for the specimen 712-cast (see Table 1), which was directly prepared from a cast button using an electric discharge machine (EDM). Tensile specimens with a gage dimension of approximately $0.7\times3\times12.7$ mm were punched from the fabricated sheets. Only one specimen (i.e. 712-a) had a smaller gage dimension of $0.3\times3\times12.7$ mm because the sheet was rolled down to 0.3 mm thickness. The punched and EDM cut surfaces of the tensile specimens were then ground using fine SiC papers prior to the subsequent heat treatments.

The alloys 200 and 712 were originally boron-free materials. However, both alloys were contaminated with boron during fabrication and annealing. The details of this contamination have been described elsewhere [17]. Briefly, the boron penetrated into the materials during (1) cross-annealing with boron-doped materials and (2) annealing in a furnace previously contaminated with boron. Also, it was discovered that the degree of boron contamination depends not only on exposure to the boron source mentioned above, but also on how many times the specimens were annealed in a furnace, or cross-annealed with boron-doped materials. As the number of annealings increases, the possibility that the specimens becomes contaminated also increases. The other parameters, such as the type of furnace used and annealing temperature and time, were also shown to affect the level of boron contamination. Fortunately or unfortunately, we were therefore able to prepare $Ni_3(Si,Ti)$ alloys with various levels of boron concentration. Table 1 lists the specimens prepared in this study and also the number of anneals given during the processing.

The grain boundary compositions of the $Ni_3(Si,Ti)$ alloys were found to depend on the final heat treatment. Also, it was observed that the cooling rate after annealing (i.e. whether water- or furnace-cooled) as well as the annealing temperature affects the composition at the grain boundaries. Selecting various heat treatment schemes as shown in Table 1, we were eventually able to prepare $Ni_3(Si,Ti)$ specimens with a wide range of boron concentration at the grain boundaries. These specimens consisted of $L1_2$ grains with average grain sizes of $50\sim70$ μm. The alloy 713 contained second phases (probably borides) not only in the grain interiors but also at the grain boundaries, and had a slightly smaller grain size than the alloys 200 and 712. It has been reported that the solubility of boron in the $Ni_3(Si,Ti)$ phase is below 50 wt ppm [1]. As for the segregated boron, it was homogeneously distributed among the grain boundaries, through the entire cross section of the specimens, although boron had penetrated (i.e.

Table 1
Specimen numbers, heat treatments and mechanical properties of the $Ni_3(Si,Ti)$ alloys used in this study

Specimen number	Number of anneals during fabrication	Heat treatment	Yield strength (MPa)		Elongation (%)		Ultimate tensile strength (MPa)	
			$8.3\times10^{-5}\,s^{-1}$	$8.3\times10^{-4}\,s^{-1}$	$8.3\times10^{-5}\,s^{-1}$	$8.3\times10^{-4}\,s^{-1}$	$8.3\times10^{-5}\,s^{-1}$	$8.3\times10^{-4}\,s^{-1}$
200-1	5	1303 K×5 h→973 K×2 h→773 K×5 h→WQ	–	626	–	36.3	–	1367
200-3	5	1303 K×5 h→1073 K×1 h→WQ	–	634	–	12.3	–	928
200-2	5	1303 K×5 h→1273 K×20 min→WQ	–	502	–	4.0	–	502
713	5	1303 K×5 h→1073 K×1 day→FC	673	666	39.4	39.3	1439	1437
712-a	> 10	1273 K×5 h→FC[a]	634	–	38.0	–	1391	–
712-2	5	1303 K×5 h→1073 K×1 day→FC[a]	654	645	41.1	39.8	1430	1419
712-6	5	1303 K×5 h→1073 K×1 day→FC	620	–	4.7	–	733	–
712-4	5	1273 K×5 h→FC	660	–	3.0	–	655	–
712-cast	1	—	–	–	–	–	–	–

[a] Cross-annealed with boron-charged alloy (specimen 713).

contaminated) from the environment [17]. An inhomogeneous boron distribution (i.e. penetration) was observed when the alloys were annealed at low temperatures (i.e. ~973 K) [17]. The mechanical properties observed in this study can be correlated with those in specimens intentionally doped with boron since the higher annealing temperatures resulted in uniform boron distributions.

Tensile tests were done in air (with the humidity ranging between 50 ± 20%) at strain rates of $8.3\times10^{-5}\,s^{-1}$ and $8.3\times10^{-4}\,s^{-1}$. The former strain rate was used mostly in the alloys 713 and 712, while the latter strain rate was used mostly in the alloy 200. The yield strength, ultimate tensile strength and tensile elongation were calculated from recorded strip charts showing displacement versus load. The fracture surfaces from selected tensile specimens were examined using a scanning electron microscope (SEM).

Auger spectroscopy was performed on small notched specimens made from the shoulder portions of the fractured specimens except for the cast material (i.e. the alloy 712-cast). A good correlation between the mechanical properties and grain boundary composition is expected from this procedure. The detailed procedures for specimen preparation and data collection have been described elsewhere [16]. Briefly, the small notched specimens were attached to tensile specimen grips quickly after cathodically charging with hydrogen at room temperature, inserted into an ultra-high vacuum fracture and introduction stage (FAIS) attached to the AES instrument [16], and then fractured. Immediately after fracture, one part of the specimen was transferred into the AES instrument without exposing to air. At least 20 areas including both transgranular and intergranular regions were analyzed on each sample (it is noted that analysis of transgranular areas is essential to obtain the correct sensitivity factor for each constituent element). The AES measurements were carried out using a 5 kV electron beam with about 160 nA current. Quantitative values of the various elements, B, Ti, Ni and Si were obtained using the 179, the 422, the 848 and the 1619 eV peaks, respectively. The sensitivity factor of boron was taken from a table supplied by the scanning Auger microscope manufacturer. The average intergranular and transgranular compositions were deduced from these measurements. Particular attention was given to the boron concentration and the parameter defined by concentrations of the constituent elements which could be correlated with the mechanical properties, i.e. the environmental embrittlement of the $Ni_3(Si,Ti)$ alloys.

3. Results

3.1. Mechanical behavior

Table 1 summarizes the yield strengths, elongations and ultimate tensile strengths of the $Ni_3(Si,Ti)$ alloys which were fabricated and heat treated in various

conditions, and then deformed in air. The specimens (1) quenched from a low annealing temperature (e.g. specimen 200-1), (2) cross-annealed with the boron-doped alloy followed by furnace cooling (e.g. specimen 712-2) and (3) intermediate-annealed more than 10 times during fabrication followed by furnace cooling (e.g. specimen 712-a) all showed high tensile elongation values. On the other hand, the specimens quenched from a high temperature (e.g. specimen 200-2) and the specimen not annealed with the boron-doped alloy followed by furnace cooling (e.g. specimen 712-6) all showed low tensile elongation values. The yield strengths measured were basically insensitive to the two testing conditions (i.e. $8.3\times10^{-5}\,s^{-1}$ and $8.3\times10^{-4}\,s^{-1}$) and the material conditions (e.g. the heat treatment and the kind of alloy whether ORNL or IMR specimens). Also, the ultimate tensile strengths are correlated well with the tensile elongations measured; high tensile elongation corresponded to high ultimate tensile strength. The intentionally boron-doped specimen 713 showed a higher tensile elongation than the similarly fabricated and heat treated specimen (i.e. 712-6). The yield strength of alloy 713 was slightly higher than those of alloys 200 and 712 probably because of the existence of a second phase (borides). However, the reduced tensile elongations should be attributed to the moisture-induced embrittlement, because the specimen quenched from 1273 K showed a low tensile elongation (~3.8%) in air but distinctly higher tensile elongation in high purity oxygen (~35.3%) [18].

Corresponding to these mechanical properties, widely different fractographies were observed, as shown in Fig. 1. The specimens quenched from a low annealing temperature (e.g. specimen 200-1) and cross-annealed with the boron-doped alloy followed by furnace cooling (e.g. specimen 712-2) showed mostly transgranular fracture, while the specimens quenched from a high temperature (e.g. specimen 200-2) and independently annealed (i.e. not in the presence of the boron-doped alloy) followed by furnace cooling (e.g. specimen 712-6) exhibited mostly intergranular fracture. Thus, the tensile elongations are well correlated with the fracture mode.

3.2. Grain boundary compositions

An SEM micrograph of the specimen 712-2 which was cathodically charged and broken in the AES instrument is shown in Fig. 2. The circumferential region consists of mostly intergranular fracture due to hydrogen penetration while the inner region consists of transgranular fracture. Although longer hydrogen charging times result in larger areas of intergranular fracture, certain areas consisting of transgranular fracture should be examined in order to obtain correct sensitivity factors for the constituent elements and to correctly calculate the grain boundary composition. The typical Auger spectra shown in Fig. 3 were obtained from intergranular areas in the specimens which displayed the highest boron peak and an intermediate boron peak in this study. The signals from oxygen and carbon in addition to the three constituent elements, Ni, Si and Ti, and the impurity (boron) were all observed. The interstitial elements of O and C are believed to be a result of contamination within the AES instrument because they were detected also on the transgranular areas.

The atomic concentrations measured for Si,Ti and B for one sample (200-1) are shown in Fig. 4. The error bars represent plus or minus one standard deviations. The average intergranular compositions are shown as atomic percents in Table 2. High amounts of boron were measured in the intentionally boron-doped specimen (713), the specimen quenched from a low annealing temperature (specimen 200-1), the specimen cross-annealed with the boron-doped alloy followed by furnace cooling (specimen 712-2) and the specimen intermediate-annealed for more than ten times during fabrication (specimen 712-a). It is interesting to note that the highest boron concentration was observed in the specimen (712-IMR) intermediately annealed for more than 10 times during the fabrication, rather than in the intentionally boron-doped specimen (713). On the other hand, low amounts of boron were observed in the specimen (200-2) quenched from a high temperature and the specimen not annealed with the boron-doped alloy followed by furnace cooling (specimen 712-6). Concerning the constituent elements, the grain boundaries in all of the specimens measured were enriched in Ni, and depleted of Si and Ti, as previously observed in $Ni_3(Si,Ti)$ alloys [16,18]. Also, two negative correlations appear to exist between Ni and Si [Fig. 5(a)], and between Ni and Ti [Fig. 5(b)], respectively; as the Ni concentration increases, the Si and Ti concentrations decrease, respectively. The R^2 value of 0.7 indicates a 70% confidence rating that a change in Si or Ti is resulting in a change in the Ni concentration.

Attempts to look for correlations between the tensile elongations and the grain boundary concentrations of the constituent elements and boron were performed. An apparent correlation was observed between the tensile elongation and the grain boundary concentration of boron, as shown in Fig. 6. The tensile elongation did not change in a monotonic fashion but showed a sharp transition; the tensile elongation was low and insensitive to the boron concentration at low levels of boron, but rapidly increased with increasing boron concentration, and was high and again insensitive to the boron concentration at high levels of boron. Consequently, there appears to be a critical grain boundary concentration of boron (i.e. c_B), above which the $Ni_3(Si,Ti)$ alloys are ductile (i.e. not susceptible to the moisture-induced

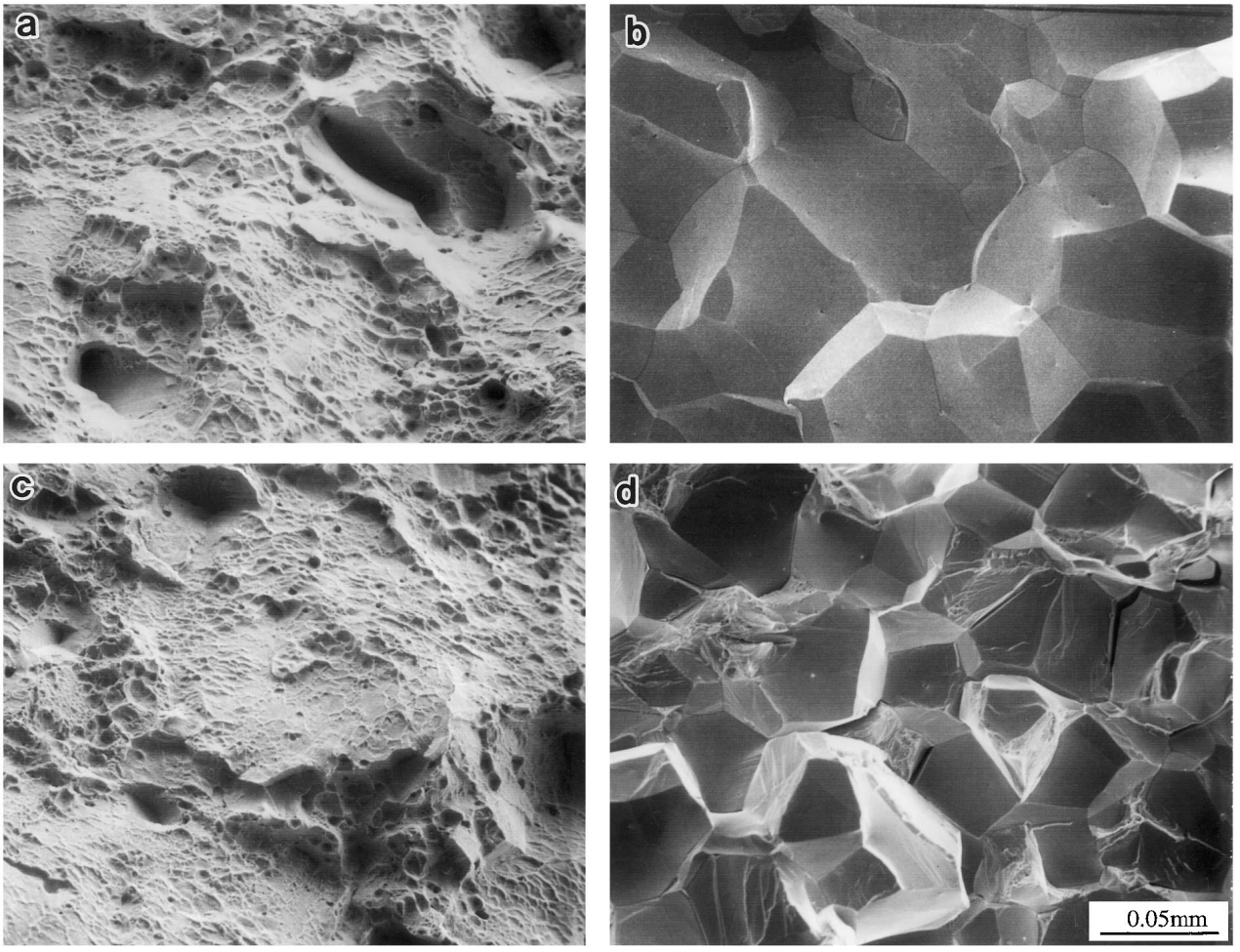

Fig. 1. SEM micrographs of the specimens quenched from (a) 773 K (specimen 200-1) and (b) 1273 K (specimen 200-2), and furnace cooled from (c) 1073 K (specimen 712-2) and (d) from 1073 K (specimen 712-6). Note that the specimen 712-2 was cross-annealed with the boron-doped specimen 713.

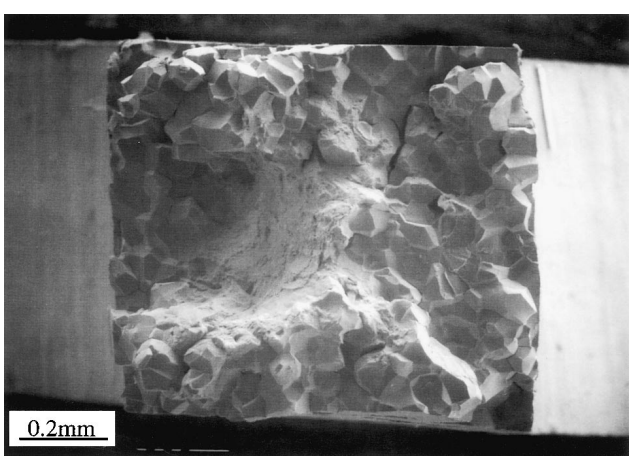

Fig. 2. SEM micrograph of the specimen 712-2 which was cathodically charged and broken in AES instrument. The specimen 712-2 was cross-annealed with the boron-doped alloy, followed by furnace cooling, as shown in Table 1. Note that the circumferential region consists of mostly intergranular fracture due to hydrogen penetration, while the inner region consists of transgranular fracture.

embrittlement). It is apparent from this plot that the critical grain boundary concentration of boron depends on the strain rate. In other words, brittle-ductile transition of the specimens deformed at $8.3\times10^{-5}\,s^{-1}$ took place at $c_B\sim2.6$ at%, while that of the specimens deformed $8.3\times10^{-4}\,s^{-1}$ took place at $c_B\sim0.8$ at%. On the other hand, no correlations were observed between the tensile elongation and the concentrations of any one of the constituent elements (Ni, Si or Ti).

In previous work [16], an embrittlement parameter defined as (Si + Ti)/Ti appeared to correlate well with the tensile elongation, where Si and Ti are the atomic concentrations of these elements at the grain boundaries. The reasoning behind the choice of this parameter was that Ti has beneficial and detrimental effects on the moisture-induced embrittlement of the $Ni_3(Si,Ti)$ alloys because Ti appears to enhance the grain boundary cohesion, as suggested by Takasugi et al. [3], and also reacts with water vapor in air and generates atomic hydrogen. On the other hand, Si while it is expected to

react with water vapor in air and generate atomic hydrogen, is ineffective in increasing the grain boundary cohesion [19]. Fig. 7 shows a plot of the tensile elongation versus the parameter, (Si + Ti)/Ti. A good correlation was observed between the tensile elongation and this parameter. Like the correlation between the tensile elongation and the grain boundary concentration of boron, the tensile elongation showed a sharp transition; the tensile elongations were low and insensitive to the value of this parameter in high ranges of this parameter, rapidly increased around the value of 2.5, and were high and again insensitive to the value in low ranges of this parameter. However, the transitions corresponding to the two different strain rates did not fall on separate curves.

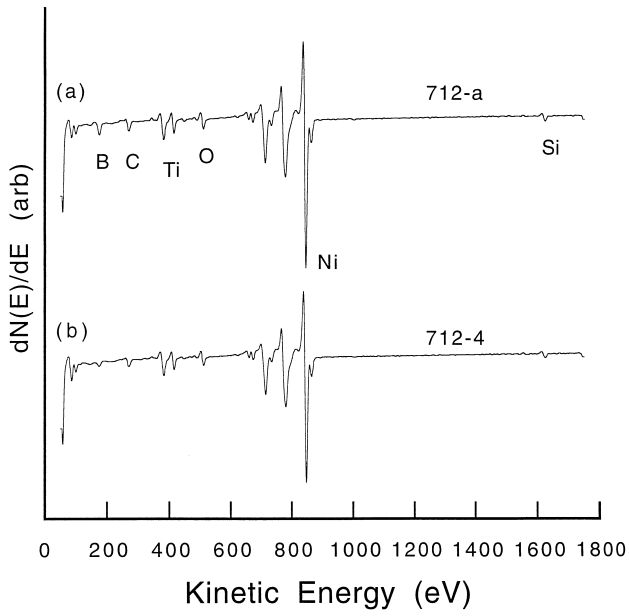

Fig. 3. Digitally smoothed and differentiated Auger spectra obtained from the grain boundary regions of the two specimens furnace-cooled from 1273 K. Note that the specimen 712-a (a) was cross-annealed with the boron-doped alloy and the specimen 712-4 (b) was separately annealed.

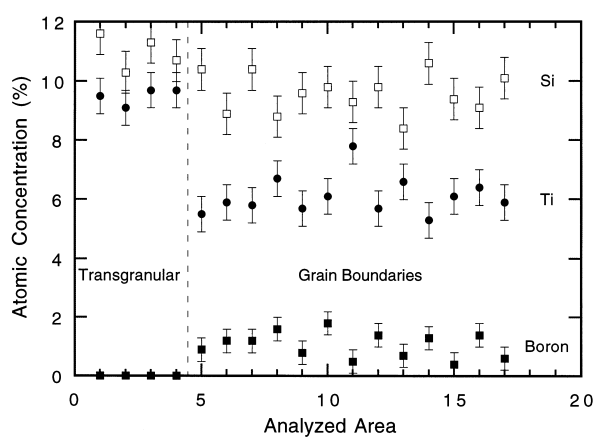

Fig. 4. Plot of the measured atomic concentrations of Si, Ti and B for all areas analyzed on sample 200-1. Error bars represent plus or minus one standard deviation.

4. Discussion

It was shown that the $Ni_3(Si, Ti)$ alloys were embrittled in air in certain conditions. These results are quite consistent with many observations published previously [3,4,6,13]. Mechanisms for environmental embrittlement of Ni_3Si [19] and $Ni_3(Si,Ti)$ [3,4,6] alloys have been proposed previously. The main cause of the environmental embrittlement of the $Ni_3(Si,Ti)$ alloys was attributed to the reaction of Si and Ti with water vapor in air according to the equation, Si(or Ti) + $2H_2O \rightarrow$ Si (or Ti)O_2 + 4H. The atomic hydrogen generated penetrates into crack tips at grain boundaries causing intergranular fracture. Both experimental and theoretical studies indicate that (1) the atomic composition at the free surface of a material may directly affect the decomposition kinetics of water vapor, and (2) the atomic composition at the grain boundaries of freshly exposed surfaces during deformation may affect the decomposition of water vapor [20]. In $L1_2$ alloys, it is also considered that absorbed hydrogen can migrate and then condense at grain boundaries, resulting in intergranular fracture. Thus, the grain boundary composition can play an extremely important role in the environmental embrittlement of the $Ni_3(Si,Ti)$ alloys as well as other $L1_2$ alloys. Therefore, it is expected that the tensile ductility in air is very sensitive to the grain boundary compositions, and small changes in the impurities (boron in this alloy) as well as the constituent elements (Ni, Si and Ti in this alloy) at the grain boundaries. Indeed, as shown in this study, the boron concentration at the grain boundaries, and also the parameter defined by the constituent elements of Si and Ti at the grain boundaries, greatly affect the tensile elongation.

It is unlikely that boron directly affects the decomposition process of water vapor at the free surface of the $Ni_3(Si,Ti)$ alloy because of its very low level. However, boron (as an impurity) was observed to enrich at the grain boundaries of the present $Ni_3(Si,Ti)$ alloys. It has been discussed that boron at these levels can have very beneficial effects on suppressing the moisture-induced embrittlement of Ni_3Al, Ni_3Si and their alloys [9], by (1) reducing the hydrogen diffusion [21], blocking site occupation of hydrogen and/or (2) reducing decomposition kinetics of water vapor [20]. It is thus expected that boron at the grain boundaries suppresses the moisture-induced embrittlement irrespective of the mechanisms proposed. The constituent element Si also plays a role in the reaction with water vapor in air, generating atomic hydrogen. On the other hand, Ti has both beneficial and detrimental effects on the moisture-induced embrittlement of the $Ni_3(Si,Ti)$ alloys by

Table 2
Average atomic compositions of the grain boundaries and transgranular regions of the $Ni_3(Si,Ti)$ alloys investigated

Specimen number	Boron	Nickel		Silicon		Titanium		(Si + Ti)/Ti	(Si + Ti-B)/Ti
	(GB)	(GB)	(TG)	(GB)	(TG)	(GB)	(TG)	(GB)	(GB)
200-1	1.1 ± 0.4	84.3 ± 0.5	79.5 ± 0.8	9.6 ± 0.7	11.0 ± 0.6	6.1 ± 0.6	9.5 ± 0.3	2.6	2.4
200-3	0.7 ± 0.4	82.9 ± 0.7	79.5 ± 0.4	10.6 ± 0.5	11.0 ± 0.4	6.5 ± 0.5	9.5 ± 0.5	2.6	2.5
200-2	0.4 ± 0.2	82.9 ± 0.8	79.5 ± 1.1	10.3 ± 0.8	11.0 ± 0.7	6.8 ± 0.4	9.5 ± 0.7	2.5	2.4
713	4.3 ± 1.5	82.7 ± 0.8	79.5 ± 0.8	10.3 ± 0.6	11.0 ± 0.7	7.0 ± 0.4	9.5 ± 0.3	2.5	1.9
712-a	7.1 ± 1.0	84.1 ± 0.5	79.5 ± 0.7	9.4 ± 0.7	11.0 ± 0.9	6.5 ± 0.4	9.5 ± 0.4	2.5	1.4
712-2	2.5 ± 1.2	83.3 ± 0.7	79.5 ± 0.5	10.2 ± 0.8	11.0 ± 0.7	6.5 ± 0.5	9.5 ± 0.4	2.6	2.2
712-6	1.2 ± 0.6	84.0 ± 0.9	79.5 ± 0.4	10.0 ± 0.8	11.0 ± 0.6	6.0 ± 0.3	9.5 ± 0.4	2.7	2.5
712-4	2.6 ± 1.2	83.7 ± 1.4	79.6 ± 0.7	10.3 ± 1.4	11.0 ± 0.8	6.0 ± 0.5	9.5 ± 0.3	2.7	2.3
712-cast	0.2 ± 0.3	82.7 ± 0.9	79.5 ± 0.8	10.4 ± 0.7	11.0 ± 0.5	7.0 ± 0.8	9.5 ± 0.4	2.5	2.5

Compositions reported as at% ± 1 SD.
GB, grain boundary; TG, transgranular.

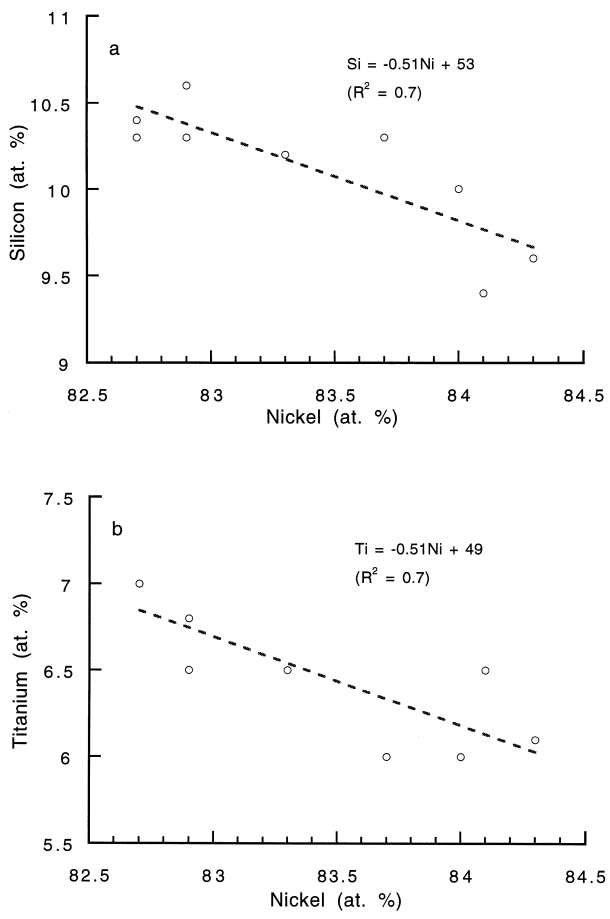

Fig. 5. Plot showing correlations in grain boundary compositions between (a) Ni and Si, and (b) Ni and Ti. The dotted lines are linear least squares fits to the data with the corresponding equations and R^2 values shown in the upper right corners of the graphs.

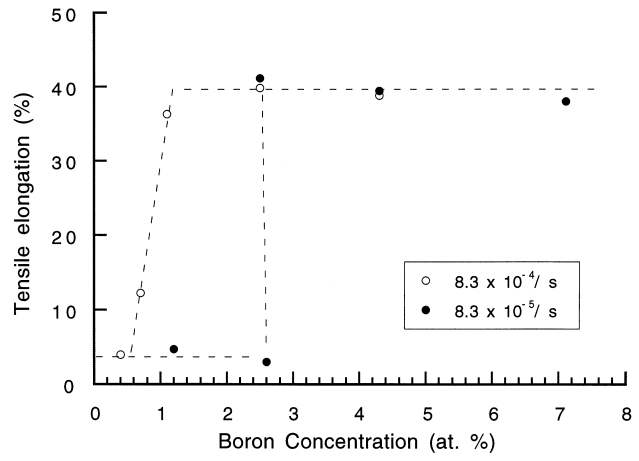

Fig. 6. Graph plotting the tensile elongation versus the grain boundary concentration of boron. Note that the data of the tensile elongation were taken in air at two different strain rates of $8.3\times10^{-5}\,s^{-1}$ and $8.3\times10^{-4}\,s^{-1}$.

enhancing their grain boundary cohesion [3] and promoting the reaction with water vapor in air, respectively. This consideration led to the parameter defined by (Si + Ti)/Ti and prediction that the tensile ductility should increase as this parameter decreases [16]. Indeed, the correlation between this parameter and the tensile elongation was observed in the previous study [16], and again in this study. However, as shown in Fig. 7, this parameter fails to separate the ductile–brittle transition (DBT) at the two different strain rates.

The results obtained in this study indicate that not only grain boundary concentration of boron but also grain boundary compositions of the constituent elements (such as Si and Ti) actually affect the moisture-induced embrittlement of the $Ni_3(Si,Ti)$ alloys. By combining these elements, a new parameter can be defined as (Si + Ti−B)/Ti. The grain boundary concentration of boron is subtracted from the numerator of the previous parameter because boron plays a role in suppressing the decomposition of water vapor, as mentioned above. Fig. 8 shows a plot of the tensile elongation versus the new parameter defined by (Si + Ti-B)/Ti. Like the correlation with the grain boundary concentration of boron, and also with the parameter (Si + Ti)/Ti, the

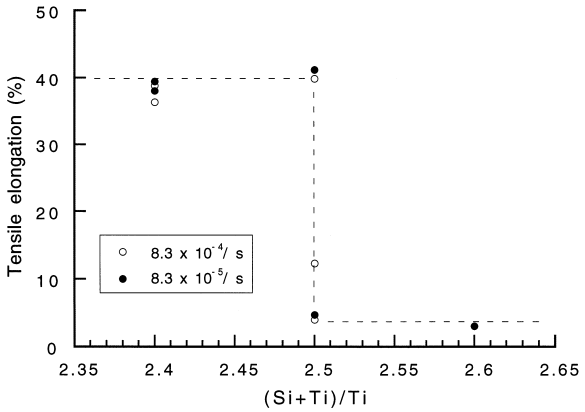

Fig. 7. Graph plotting the tensile elongation versus the parameter defined by (Si + Ti)/Ti. Note that the data of the tensile elongation were taken in air at two different strain rates of $8.3\times10^{-5}\,s^{-1}$ and $8.3\times10^{-4}\,s^{-1}$.

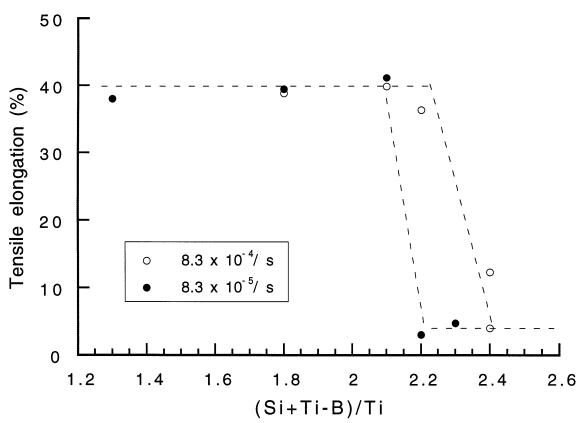

Fig. 8. Graph plotting the tensile elongation versus the parameter defined by (Si + Ti-B)/Ti. Note that the data of the tensile elongation were taken in air at two different strain rates of $8.3\times10^{-5}\,s^{-1}$ and $8.3\times10^{-4}\,s^{-1}$.

tensile elongation showed a sharp transition. It is important to point out that, in this case, the two transitions corresponding to the two strain rates are clearly distinguished; the transition at the slower strain rate takes place at a smaller value of this parameter than that at the higher strain rate. It appears that this parameter is better than the previous parameter (Si + Ti)/Ti in defining the transition. Also, considering the gentle slope of this transition, this parameter is even better than boron concentration in defining the transition.

As shown in Figs. 6 and 8, sharp brittle–ductile transitions were observed at both the strain rates used. Critical grain boundary concentrations of boron corresponding to these transitions were ~2.6 and ~0.8% at strain rates of $8.3\times10^{-5}\,s^{-1}$ and $8.3\times10^{-4}\,s^{-1}$, respectively. Similarly, critical values of the parameter (Si + Ti-B)/Ti were ~2.2 and ~2.4 at strain rates of $8.3\times10^{-5}\,s^{-1}$ and $8.3\times10^{-4}\,s^{-1}$, respectively. At a slower strain rate, higher grain boundary concentrations of boron are required to prevent the harmful action of hydrogen atoms at the grain boundaries and to obtain higher tensile elongation. A possible reason for this is that at a slower strain rate more hydrogen atoms are generated and more time is available for the hydrogen to penetrate along the grain boundaries.

It is finally noted that the observed tensile elongations were never zero, but mostly 3~5% under the influence of hydrogen. This result is quite different from those of the binary Ni_3Si [19] and Ni_3Al alloys [9]. This difference may be attributed to the constituent element Ti which plays a beneficial role in intergranular fracture; that is, Ti enhances intrinsic grain boundary cohesive strength even under the influence of hydrogen [3].

5. Conclusions

The mechanical properties and grain boundary chemistries of the $Ni_3(Si,Ti)$ alloys containing widely different levels of boron were studied in air at room temperature, using tensile testing, SEM and AES. The following conclusions were obtained from the present study.

1. Different tensile elongations and fracture modes were observed, depending on the fabrication procedure, heat treatment and strain rate. Higher tensile elongations were accompanied by transgranular fracture, while lower tensile elongations were accompanied by intergranular fracture.
2. Boron was observed to be enriched at the grain boundaries and widely different grain boundary concentrations of boron were observed, depending on the fabrication procedure and heat treatment. Silicon and titanium were depleted, while nickel was enriched at the grain boundaries in all the specimens observed.
3. The tensile elongation was correlated well with the grain boundary concentration of boron and also with the parameter defined by (Si + Ti−B)/Ti. A sharp brittle–ductile transition occurred as the grain boundary concentration of boron increased or the parameter (Si + Ti−B)/Ti) decreased. The critical grain boundary concentrations corresponding to this transition were determined to be sensitive to the strain rate.

Acknowledgements

This research was sponsored by the Division of Materials Sciences, US Department of Energy, under contract DE-ACO5-96OR22464 with Lockheed Martin Energy Research Corporation, and also in part by the

ISIJ Research Promotion Grant, Japan (TT). The authors are grateful to JL. Wright for his technical assistance.

References

[1] Takasugi T, Shindo D, Izumi O, Hirabayashi M. Acta Metall et Mater. 1990;38:739.
[2] Ochiai S, Oya Y, Suzuki T. Acta Metall 1984;32:289.
[3] Takasugi T, Nagashima M, Izumi O, Acta Metall et Mater 1990;38:747.
[4] Takasugi T, Izumi O, Yoshida M. J Mater Sci 1991;26:1173.
[5] Takasugi T, Watanabe S, Izumi O, Fat-Halla NK. Acta Metall et Mater 1989;37:3425.
[6] Takasugi T, Suenaga H, Izumi O. J Mater Sci 1991;26:1179.
[7] Takasugi T. In: Stoloff N, Duquette DJ, Giamei AF, editors. Critical issues in the development of high temperature structural materials. Warrendale (PA): TMS, 1993. p. 399.
[8] Liu CT. In: Liu CT, Cahn RW, Sauthoff G, editors. Ordered intermetallics—physical metallurgy and mechanical behavior. Dordrecht (The Netherlands): Kluwer Academic, 1992. p. 321.
[9] Liu CT, George EP. In: Deevi C, Sikka VK, Maziasz PJ, Cahn RW, editors. International Symposium on Nickel and Iron Aluminide; Processing, Properties, and Applications. Materials Park (OH): ASM, 1997. p. 21.
[10] Takasugi T, Yoshida M. J Mater Sci. 1991;26:3032.
[11] Ma CL, Takasugi T, Hanada S. Materials Trans JIM 1995;36: 30.
[12] Takasugi T, Hono K, Suzuki S, Hanada S, Sakurai T. Scripta Metall et Mater 1993;29:1587.
[13] Ma CL, Takasugi T, Hanada S. Scripta et Mater 1995;32: 1025.
[14] Ma CL, Takasugi T, Hanada S. High temperature ordered intermetallic alloys VI, vol. 364. Pittsburgh, (PA) MRS Symposium Proceedings Publications, 1995. p. 1159.
[15] Kumar KS, Liu CT, Wright JL. Intermetallics 1996;4:309.
[16] Heatherly L, George EP, Liu CT, Kumar KS. Materials Science and Eng A, in press.
[17] Takasugi T, Liu CT, Heatherly L, Lee E, George EP. Intermetallics 1998;8:369.
[18] Takasugi T, Liu CT, Lee E, Heatherly L, George EP. Scripta Materialia 1998;38:287.
[19] Liu CT, George EP, Oliver WC. Intermetallics 1996;4:77.
[20] Lee KH, Lukowski JT, White CL. Scripta met et mater 1996;35:1153.
[21] Wan XJ, Zhu JH, Jing KL, Liu CT. Scripta metall et mater 1994;31:677.